

## On End-Effect Correction for Couette Type Viscometers for Newtonian and Non-Newtonian Fluids

Rune W. Time<sup>1</sup>, Herimonja A. Rabenjafimanantsoa<sup>1</sup>, Vassilios C. Kelessidis<sup>2</sup>, and Roberto Maglione<sup>2</sup>

<sup>1</sup> University of Stavanger, Norway

<sup>2</sup> Technical University Crete, Chania, Crete – Greece

### ABSTRACT

Analysis and experimental investigations are presented on end-effects for rotating cylinder viscometers used extensively for Newtonian and non-Newtonian fluids. Such viscometers have already embedded at manufacturing stage an end-effects correction and give directly the shear stress which does not allow end-effect quantification in a straight forward manner. Experiments with Newtonian and non-Newtonian fluids show that there is no additional end-effect from the bottom of the stationary bob. In this joint research project between TUC and UiS it is shown that here are additional end-effects contribution from the top section of the bob which has not been taken into account in the design and manufacturing of the instrument.

### INTRODUCTION

Data analysis and rheological parameter estimation for Newtonian and non-Newtonian fluids using rotating cylinder viscometers is normally done with the assumption that there is a narrow gap between the cylinders, in particular for the viscometers used extensively in oil-field industry<sup>1</sup>. Implicit assumptions involve also Newtonian velocity profile for the flow between the two cylinders and that the cylinders are infinitely long. The former assumption has been questioned by several

investigators for rheological measurements of non-Newtonian fluids, even for narrow gap instruments<sup>2,3-5</sup>. The latter, known as the end effects problem, has been questioned not only for non-Newtonian<sup>6,7</sup> but also for Newtonian fluids<sup>8-10</sup>. If end effects are present, the additional torque from top and/or bottom of the bob could be determined with an extra depth of immersion<sup>11-13</sup>, thus,

$$T = 4\pi \cdot (h + \Delta h) \cdot R_i^2 \cdot \left( \frac{\delta^2}{\delta^2 - 1} \right) \mu \cdot \Omega \quad (1)$$

with  $\Delta h$  depending on  $R_0, R_i, h$  as well as on the distance from the bottom of the cup  $L$ <sup>14</sup>.

Oil-field viscometers are direct-indicating<sup>15</sup>, giving directly the shear stress and the rheological parameters but not the torque, which presents a problem for using above equation. They have been specially manufactured so that end-effects are taken care of through appropriate design and manufacturing of the instrument, the ‘embedded’ correction. The overall correction is achieved with a calibration, performed only with a Newtonian fluid. Quantification of end-effects for non-Newtonian fluids with oil-field viscometers has been attempted only by<sup>6,15</sup>, but also in a recent theoretical paper for measurement of

fresh concrete<sup>17</sup> involving numerical and analytical solution of the fluid flow field.

Interestingly enough, there is no indication in the paper of Savins and Roper<sup>15</sup> concerning the existence of the top conical section of the bob in the viscosity measurement, except with respect to the determination of gel strength of the fluid, where the extra length is taken into account by letting the total bob length as,

$$h_{eq} = h + h_{cone} / 3 \quad (2)$$

The torque on the bob can be estimated by,

$$T = 2\pi R_i^2 h_{eq} \tau \quad (3)$$

where  $h_{eq}$  is the equivalent length that includes end-effect corrections from the bottom section and the top sections, i.e.  $h_{eq} = h + \Delta h$ . It must be stressed that the value of  $h_{eq}$  is nowhere indicated, neither in any of the supporting papers nor on any manuals of the direct indicating viscometers, rather, the length of the cylindrical part,  $h$ , (38.00 mm) is only indicated. Kelessidis et al.<sup>16</sup> have suggested a procedure for the estimation of  $h_{eq}$ . When the instrument is calibrated with a Newtonian fluid of known viscosity  $\mu_1$  and rotates at a particular speed, corresponding to a shear rate  $\dot{\gamma}$ , the direct reading of  $\tau_1$  corresponds to,

$$T_1 = 2\pi R_i^2 h_{eq} \tau_1 = 2\pi R_i^2 h_{eq} \mu_1 \dot{\gamma} \quad (4)$$

When using unknown fluid of,  $\mu_2$ , at  $\dot{\gamma}$ , then,

$$\tau_2 = \frac{T_2}{C} = \frac{T_2}{2\pi R_i^2 h_{eq}} = \frac{T_2}{T_1} \mu_1 \dot{\gamma} \quad (5)$$

and hence,

$$\mu_2 = \mu_1 \frac{T_2}{T_1} \quad (6)$$

This holds true only if  $h_{eq}$  is the same for both measurements. When measuring fluid with,  $\mu_3$ , to determine whether there is an end-effect, at different heights,  $h_i$ , then the instrument measures  $T_3$ , but outputs,  $\tau_3$ , which results from a computation of the form,

$$\tau_3 = \frac{T_3}{2\pi R_i^2 h_{eq}} = \frac{T_3}{T_1} \mu_1 \dot{\gamma} \quad (7)$$

while in fact, the true shear stress, related to  $h_i$  should have been,

$$\tau'_3 = \frac{T_3}{2\pi R_i^2 h_i} = \frac{T_3}{2\pi R_i^2 h_{eq}} \frac{h_{eq}}{h_i} = \left( \frac{T_3}{T_1} \right) \left( \frac{h_{eq}}{h_i} \right) (\mu_1 \dot{\gamma}) = \left( \frac{h_{eq}}{h_i} \right) (\tau_3) \quad (8)$$

The torque could then be recomputed, so that the normal approach can be followed, i.e. plotting  $(T - h)$  to determine any end-effects, by

$$T_3^{comp} = 2\pi R_i h_i \tau'_3 = 2\pi R_i h_i \frac{h_{eq}}{h_i} \tau_3 = 2\pi R_i h_{eq} \tau_3 \quad (9)$$

Eq. 9 outlines the problem associated with the direct-indicating viscometers with respect to the end-effect determination procedures, which is the fact that the torque developed along the bob surface cannot be recovered. Thus, it cannot be verified whether there is an end-effect following the standard procedure, in direct-indicating viscometers, because the actual height is cancelling out. To overcome such problem, Kelessidis et al.<sup>16</sup> assumed that the shear stress, at a given rotational speed of the viscometer, can be written as follows:

$$\tau = \tau_{bot} + \tau_{bob} + \tau_{cone} + \tau_{rod} \quad (10)$$

where,  $\tau_{bot}$  is the shear stress developed by the fluid within the volume between the bottom of the bob and the bottom of the cup;  $\tau_{bob}$  is the shear stress developed by the fluid within the annular gap between the bob and the rotating cup;  $\tau_{cone}$  is the shear stress developed by the fluid within the annular gap between the wall of the rotating cup and the conical section of the upper part of the bob; and  $\tau_{rod}$  is the shear stress developed by the fluid in the annular gap between the wall of the rotating cup and the wall of the rod holding the bob.

They further assumed that the bottom, the cone and the rod sections can have an axial shear stress gradient,  $\xi$ , which is the same. Hence, Eq. 10 can be rewritten as follows,

$$\tau = \xi \Delta h_{bot} + \xi h_{bob} + \xi \Delta h_{cone} + \xi \Delta h_{rod} \quad (11)$$

Kelessidis et al.<sup>16</sup> have followed the above approach and using semi-theoretical arguments and experimental results for Newtonian and non-Newtonian fluids (bentonite dispersions) have determined that the overall end-effects correction represented 6.69% of the bob cylindrical length and the sought equivalent length of the bob,  $h_{eq}$  should then be 40.541 mm, instead of the proposed one of 38 mm.

They further determined that additional end-effects exists both for Newtonian and non-Newtonian fluids, with experimental results showing errors between 6.0% for the highest rotational speed and 12.0% for the lowest rotational velocity, thus giving an overall end-effect correction ranging between 12.0% and 18.0%, which compared very well with the value of 17.0% reported by Savins and Roper<sup>15</sup>. The presented work attempted to get a much better insight of the

flow patterns around the cone area, the bottom of the bob and along the bob, using the visualization techniques, to verify, qualitatively and possibly quantitatively, that the assumptions made were on the right track.

## FLOW VISUALIZATION

The model for shear stress over the cone and rod relies on having essentially the same tangential flow as in the narrow gap. In order to check the validity of the assumption, a parallel study was carried out to visualize the internal flow between the rotating outer cylinder and the static parts. An OFITE 900 rheometer was used for this experimental analysis.

### Transparent parts

A high quality transparent rotor was made in acrylic with exactly the same dimension as the original part. Two different stators were also made, one transparent acrylic and one in white teflon as shown in Fig. 1.



Figure 1. Rotor and stators in acrylic and teflon together with original stainless steel stator.

The acrylic stator allows viewing both the front and backside flow and is well suited for Particle Image Velocimetry (PIV) studies as well, since it creates very little backlighting into the flow. The white stator

is suitable for recording separately the flow on the front side, without being disturbed by the flow from the back side.

The stator radius is  $R_i = 17.245$  mm while the inner rotor radius is  $R_o = 18.415$  mm.

Image acquisition

For the recordings a NanoSense MKIII-plus camera (by DantecDynamics) with resolution 1.3 megapixel (1280x1024) was used. It has 8GB internal memory and was controlled via a laptop using the USB interface option. With full pixel resolution 6557 frames can be recorded at a speed of 1000 frames per second (fps). For the fastest rheometer speeds (600rpm) this was needed to capture all details. However 60 - 100 fps sampling rate was sufficient to capture relevant details at 10 – 100 rpm which was studied in most cases.

Adding color dye for flow visualization

In order to visualize the flow inside the rotor two optical techniques were considered; PIV analysis, and dye induced path lines or timelines. PIV would be desirable to quantify the velocity profile over the cone. Some initial tests showed that equipment rebuilding would be necessary to image the tangential flow field. So it was decided for this study to use the path line approach. It is simpler and also enables straightforward recording of the flow development in time.

The dye (water based black ink) was added with a syringe as seen in Fig. 2. The dye was allowed to settle in the narrow gap for some seconds before the rotation was started.

Experiments

A comprehensive series of experimental images were recorded to monitor the internal flow in the gap and over the conic section of the stator bob. Deionized water and Polyanionic Cellulose (PAC) were used, in PAC 50 ppm and 400 ppm

concentrations. The viscosity for the PAC solutions is shown in Fig. 3.

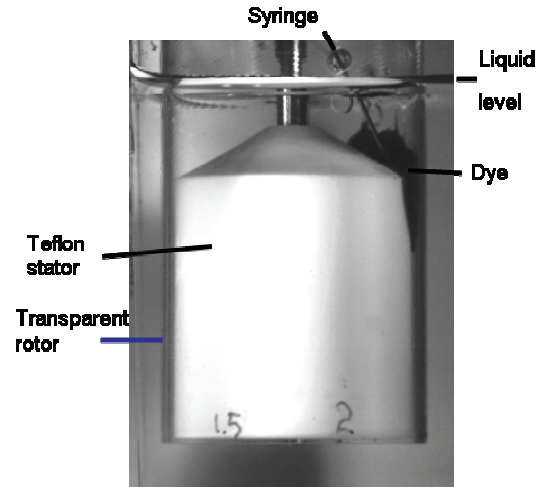


Figure 2. Color dye injection with a syringe through the venting holes of the rotor. Numbers are marked onto the rotor to visualize its motion.

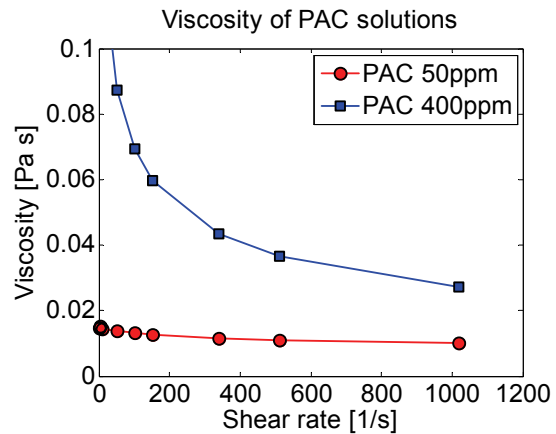


Figure 3. Viscosity versus shear rate of the PAC 50 ppm and 400 ppm solutions.

Fig. 4 shows the time development after start of rotation in water using the white teflon stator. A special "strobing" technique has been used for the representation. All the frames show the rotor subsequently at the same phase of rotation, as may be seen by the position of the numbers.

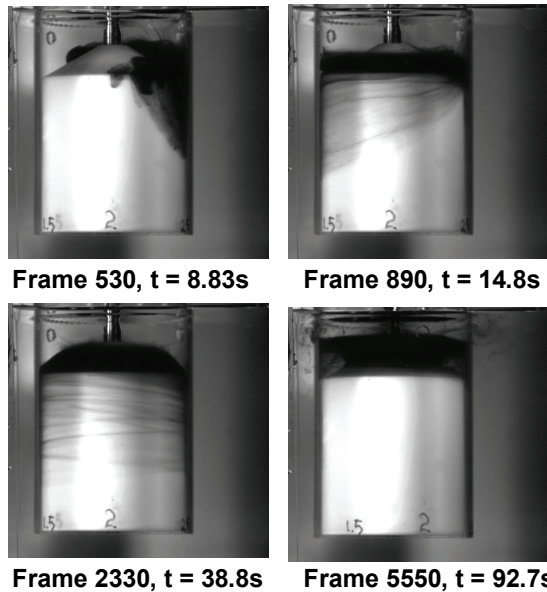


Figure 4. Time development of the flow of water in annulus and over the cone section. Water experiments at 10 rpm rotation.

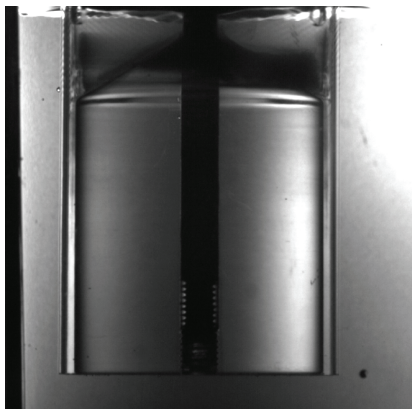


Figure 5. Transparent stator and strong back illumination reveals the flow (of water with color dye) in the narrow annulus. The stator rod is seen through the acrylic bob.

The narrow annulus gap is seen well using back lighting and opaque screen in Fig. 5. The stator rod is seen through the acrylic.

#### Water experiments

Water flows up in the annular gap and seems to follow two separate paths. One is up along the inner rotor wall directly out of the venting holes. Another flow comes from

split at the top of the annulus gap to flow upwards along the cone wall. Here it creates secondary flows as rolls and cusps as can be seen on top of the dye in figure 4 frame 2330. This kind of behaviour influences the boundary conditions for flow around cone and rod. Measuring the tangential flow profile could have revealed in more detail how much this changes the shear stress.

#### Experiments with PAC 50ppm

When PAC is added there are more pronounced structures in the volume over the cone. An effect which could resemble Weissenberg climbing creates collarlike or doughnut structures as seen in the right image in Fig.6. Rotation speed is 10 rpm.

A nice effect seen in most of the experiments with non-Newtonian flow is the slightly distorted return of dye flow structures after every two rotations of the outer cylinder. This is shown in Fig. 7 for PAC50ppm.

The distortion is small in these images with rotation speed 10 rpm. Notice the combined tangential shear and the axial compression.

#### Experiments with PAC 400ppm

Structural coherence over time increases considerably using 400 ppm PAC compared to in the 50 ppm experiments. This is shown in Fig. 8. The dye accumulates in the volume over the cone and winds up in a layered collar structure until it eventually becomes so entangled that no more structures are seen. Finally the dye reaches the rotor and comes out the venting holes, but clinging to the outside rotor wall by Weissenberg effect.

The left picture is recorded at speed 10 rpm, while in the picture to the right the rotation speed is 100 rpm, turned on after frame 3630.

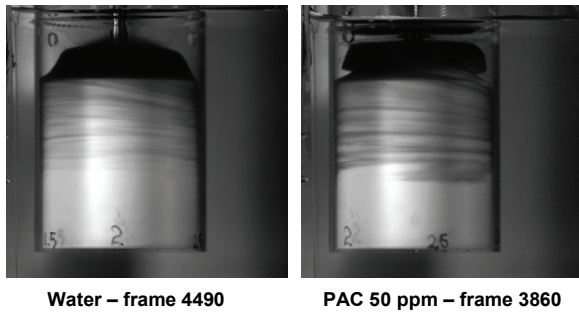


Figure 6. Comparison of PAC 50 ppm with water experiments. PAC winds the color dye into a collar, much more pronounced than with water. Rotation speed is 10 rpm.

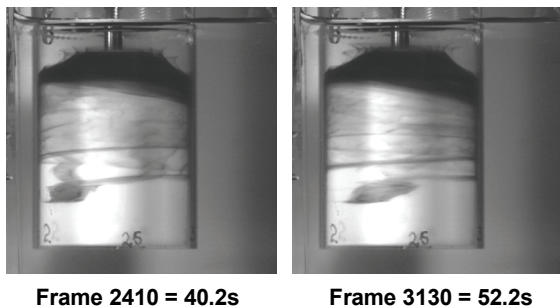


Figure 7. Dye structures return after exactly two rotor revolutions. PAC 50 ppm experiments. Rotation speed 10 rpm.

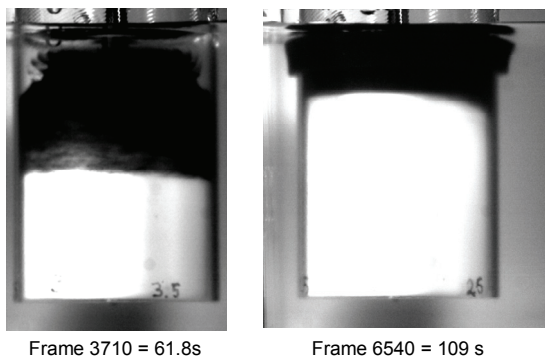


Figure 8. PAC 400 ppm after 61.8 and 109 seconds. The dye forms coherent structures before finally mixed over the whole cone zone before it flows out the holes. The dye clings outside the rotor by Weissenberg effect, as seen in the right picture.

### Analysis and interpretation

A limited PIV analysis was carried out based on the camera recordings. However the images are dominated by background objects so the reconstruction becomes biased. The use of dye and pathlines gives better result since it allows for simplified PTV (particle tracking velocimetry) in addition to contain flow history over fairly long intervals. All experiments show that there is a net inflow of fluid from the bottom of the annulus gap up to the cone area.

Using dye techniques to reveal flow structures without influencing the flow should ideally involve neutral density particles with low concentration. This might conflict with amount of colour needed for good contrast, and dense slurries will normally also modify the rheology of the flow (e.g. Kaiser et al.<sup>18</sup>). The ink particles used here however are very small, typically less than 10 micron, quickly diluted and modify the viscosity and flow pattern little.

Analysis of the experiments indicates several modifications of a pure tangential flow field. Firstly there is an active "pump" mechanism creating upward axial velocity components, although small. More important is perhaps the three-dimensional flow pattern over the cone and rod section. These secondary flows are found to vary both with fluid viscosity and with rotor speed. Secondary flows modify the boundary layers and may thus influence wall shear stress, but the overall contribution remains to be measured exactly.

### CONCLUSION

The term "end-effects" in rotating cylinder viscometer measurements incorporates both the geometry aspects of rotor and stator, but most likely also secondary flows with combined axial and tangential components. These might be referred to as "flow regime effects". This has normally been reserved for instabilities like Taylor-Couette rolls when the inner cylinder rotates or for transition to

turbulence. The theoretical analysis in the first part of the paper deals with first modifications under the assumption of a pure tangential field with axial gradient in the conic section. The flow visualization in the second part indicates that further studies should be done to clarify if also changes in boundary conditions can affect the accuracy.

## REFERENCES

1. Bourgoyne A.T., Chenevert M.E., Millheim K.K., and Young F.S. (1991), "Applied drilling engineering", SPE Textbook series, Vol. 2.
2. Joye, D.D. (2003), "Shear rate and viscosity corrections for a Casson fluid in cylindrical (Couette) geometries", *J. Colloid Interface Sci.*, **267**, 204-210.
3. Kelessidis, V.C., Maglione, R., Tsamantaki, C, and Aspirtakis, Y. (2006), "Optimal determination of rheological parameters for Herschel-Bulkley drilling fluids and impact on pressure drop, velocity profiles and penetration rates during drilling", *J. Petrol. Sci. Eng.*, **53**, 203-224.
4. Kelessidis, V.C., Tsamantaki, C., and Dalamarinis, P. (2007), "Effect of pH and electrolyte on the rheology of aqueous Wyoming bentonite dispersions", *App. Clay Sci.*, **38**, 86-96.
5. Kelessidis, V.C. and Maglione, R. (2008), "Shear rate corrections for Herschel-Bulkley fluids in Couette geometry", *Appl. Rheol.* **18**:3, 34482-1-34482-11.
6. Gucuyener, H., Kok, M.V., and Batmaz, T. (2002), "End effect evaluation in rheological measurement of drilling fluid using Couette coaxial cylinder viscometer", *Energy Source*, **24**, 441-449.
7. Savaramand, S., Carreau, P.J., Bertrand, F., Vidal, D.J.-E., and Moan, M. (2003), "Rheological properties of concentrated aqueous silica suspensions: Effects of pH and ions content", *J. Rheol.* **47**, 133-1149.
8. Lindsley, C.H. and Fischer, E.K. (1947), "End-effect in rotational viscometer", *J. Appl. Physics*, **18**, 988-996.
9. Oka, S. (1960), "Rheology: theory and applications", Academic Press, New York.
10. Barnes, H.A., Hutton, J.F. and Walters, K., (1993). "An Introduction to rheology", Elsevier, Amsterdam.
11. Van Wazer, J.R., Lyons, J.W., Kim, K.Y., and Colwell, R.E. (1963), "Viscosity and flow measurement. A laboratory handbook of rheology", Interscience Publishers, London.
12. Whorlow, R.W. (1980), "Rheological techniques", Wiley & Sons, New York, 1980.
13. Lindsay, W.J. (1990), "Principles of polymer engineering rheology", Wiley & Sons, New York.
14. Macosko, C.W. (1994), "Rheology: Principles, Measurements, and Applications", Wiley-VCH, New York.
15. Savins, J.O. and Roper, W.F. (1954), "A direct-indicating viscometer for drilling fluids, API Drilling and Production Practices", Presented at the Southwestern District, Division of Productions, Houston, March 1954, pp. 7-22.
16. Kelessidis, V.C., Maglione, R., Bandelis, G. (2009), "On the end-effect correction for Couette type oil-field direct-indicating viscometers for Newtonian and non-Newtonian fluids", *J. Petr. Sci. Engr.* **Submitted**.
17. Wallevik J.E. (2008), "Minimizing end-effects in the coaxial cylinders viscometer: Viscoplastic flow inside the ConTec BML Viscometer 3", *J. Non-Newton. Fluid Mech.* **155**, 116-123.
18. Kaiser, A.E., Grahama, A.L., and Mondy, L.A. (2004), "Non-Newtonian wall effects in concentrated suspensions", *J. Non-Newton. Fluid Mech.*, **116**, 479-488.